of HCMV was amplified (95°C for 25 s, 42°C for 15 s, and 72°C for 60 s; 40 cycles) with the following primers: AAGCTTGTGTTTTCGAACAT and TTTATTGTTCTGTCTCCTCTC [J. A. Nelson, B. Fleckenstein, G. Jahn, D. A. Galloway, J. K. McDougall, *J. Virol.* **49**, 109 (1984)]; or for the *IE2* region, TCCTCCTGCAGTTCGGCTTC and TTTCATGATATTGCGCACCT [E. S. Huang and T. F. Kowalik, in (*3*), vol. 2, p. 247]. Each 100-μl reaction mixture contained 50 mM tris-HCl (pH 9.0), 3 mM $MgCl_2$, 40 pmol of each primer, 200 μM of each deoxynucleotide triphosphate, 5 U of Amplitaq (Cetus), and 50 ng of genomic DNA.

16. T. Albrecht, I. Boldogh, M. P. Fons, T. Valyin Nagy, in (*3*), vol. 2, chap. 19.
17. C. Hagemeier *et al.*, *J. Virol.* **66**, 4452 (1992).
18. R. M. Stenberg *et al.*, *ibid.* **63**, 2699 (1989).
19. G. P. Zambetti *et al.*, *Genes Dev.* **6**, 1143 (1992).
20. The coding region of p53 was cloned into pAcUW51 (Pharmigen) baculovirus transfer vector under control of the p10 promoter. The coding region of HCMV IE84 was cloned into pVL 1392 (Pharmigen) vector under control of the polyhedrin promoter. *Spodoptera frugiperda* (Sf9) cells were grown at 27°C in Graces media (Gibco) containing 10% heat-inactivated fetal bovine serum (FBS). The Invitrogen XPRESS SYSTEM was used for transfection and generation of high-titer virus stock. The Sf9 cells (2 × 10^7 per 100-mm dish) were infected with recombinant viruses, harvested 72 hours later, and lysed in 0.4 ml of lysis buffer [50 mM tris-HCl (pH 8.0), 150 mM NaCl, 0.5% NP-40, leupeptin (25 mg/ml), and 0.35 mM phenylmethylsulfonyl fluoride]. Lysates were clarified by centrifugation and used for immunoprecipitations.
21. Lysates (~400 μg) were incubated at 4°C overnight with 1 μg of antibody 1801, and the antigen-antibody complexes then collected with protein A–Sepharose CL-4B (Pharmacia). Pellets were washed in lysis buffer, resuspended in 40 μl of loading buffer, and subjected to electrophoresis on an SDS-polyacrylamide gel. The separated proteins were transferred to a nitrocellulose filter, which was then incubated at 4°C overnight in TBST [10 mM tris (pH 8.0), 150 mM NaCl, and 0.05% Tween 20] plus 5% nonfat dry milk. The filter was incubated for 2 hours with an IE84-specific antibody (12E2; 1 μg/ml), washed in TBST, and then re-incubated with a sheep antibody to mouse immunoglobulin G (IgG) coupled to horseradish peroxidase (1:25,000 dilution). After further washes, the filter was developed with an EcL detection kit (Amersham).
22. J. J. Tumilowicz *et al.*, *J. Virol.* **56**, 839 (1985).
23. I. Gurevich, *Heart Lung* **21**, 85 (1992).
24. Fresh atherectomy specimens were obtained in the catheterization laboratory from 60 patients with restenosis. Tissue fragments (1 to 5 mg) were embedded in freezing compound, frozen in isopentane–dry ice, and cut into 10 to 20 sections of 6 μm each; two sections of 50-μm thickness were cut for DNA isolation and PCR [P. H. Gumerlock, U. R. Poonawallee, F. J. Meyers, R. W. D. White, *Cancer Res.* **51**, 1632 (1991)]. Sections were placed on polylysine-coated slides and stored at −80°C until processed for staining. The sections were thawed at 22°C, fixed in −20°C methanol, air-dried for 30 min, rehydrated in phosphate-buffered saline (PBS), and processed as in E. Speir *et al.* [*Circ. Res.* **71**, 251 (1992)]. The first and second sections were stained with hematoxylin-eosin and Movat pentachrome, respectively. Subsequent sections were stained with the following antibodies to p53: monoclonal PAb 1801, -421, and -240 at 2 μg/ml (Oncogene Science, Uniondale, NY) and polyclonal CM1 at 1:1000 [C. A. Midgley *et al.*, *J. Cell Sci.* **101**, 183 (1992)]. For nonimmune controls we used mouse myeloma protein Mopc21 (Cappel, Durham, NC) and normal rabbit serum (Sigma).
25. SMCs (passage 5, grown from explants of a 1-cm segment of human coronary artery obtained at autopsy of an 18-year-old trauma victim, from National Disease Research Interchange, Philadelphia, PA) were seeded at 20,000 cells per well in eight-chamber glass slides (Nunc) and grown in Medium 199, 20% FBS, 1% antibiotic-antimycotic for 72 hours. After removal of the medium, the cells were infected with 50 μl of viral supernatant for 2 hours. The virus suspension was then removed and replaced with 0.4 ml of growth medium. Four wells each of infected or uninfected controls for each time point were analyzed by immunocytochemistry. Cells were fixed, incubated with monoclonal antibodies 6E1 (to IE72) or 12E2 (to IE84) (Vancouver Biotech.) or with p53-specific antibodies 1801 or 421 overnight at 4°C, then reacted with biotinylated goat antibody to mouse IgG and ABC complex (Vector Labs) and with diaminobenzidine [E. Speir *et al.*, in (*24*)]. Whereas IE72 expression was maximal at 48 hours after infection and then declined, IE84 expression was low at 48 hours but was apparent in 70% of the infected cells at 7 days and in 100% of the cells at 14 days after infection.
26. For indirect immunofluorescence, human coronary SMCs at passage 5 were seeded at 30,000 per square centimeter in eight-well glass chamber slides in Medium 199 and 10% FBS and grown for 48 hours. After three washes with warm PBS, cells were fixed in 1% paraformaldehyde for 2 min, then in 50% acetone-methanol at −10°C for 7 min. Cells were then air-dried, washed in PBS, and blocked with 1% goat serum (Vector Labs) for 20 min. Antibody 12E2 (50 μl), diluted 1:200 in 0.1% crystalline bovine serum albumin (BSA), was added to the wells for 1 hour at 22°C. Cells were washed in warm PBS and the lissamine-rhodamine conjugated goat secondary antibody (Jackson ImmunoResearch, West Grove, PA; diluted in 1% rabbit serum in PBS at 1:50) was added for 30 min at 37°C. Cells were again washed with warm PBS and polyclonal antibody CM1 (Signet, Dedham, MA; diluted 1:200 in 0.1% BSA) was added to the wells for 1 hour at 22°C. Cells were washed in PBS, fluorescein isothiocyanate-conjugated secondary antibody [diluted in 1% rabbit IgG in PBS (Vector Labs) at 1:50] was added for 30 min, and the cells were washed again. Finally, cells were mounted in 0.1% *p*-phenylenediamine dissolved in PBS (pH 8), and adjusted with carbonate buffer (pH 9.0).
27. The complete coding region of *IE2* was PCR-amplified from complementary DNA (cDNA) and cloned into the pRc/RSV expression vector with Hind III and Xba I linkers. Human coronary SMCs were grown in Medium 199 and 10% FBS for 48 hours, then synchronized with 5 mM thymidine for 24 hours [E. Speir and S. E. Epstein, *Circulation* **86**, 538 (1992)] and transiently transfected by lipofection (Dotap, Boehringer) with 2 μg of each plasmid and 1 μg of the reporter plasmid p50-2. The results are the average CAT activity of duplicate samples. Three separate transfections were performed. Cell extracts were prepared by three freeze-thaw cycles and then measured for CAT activity with [^{14}C]chloramphenicol and butyryl coenzyme A [T. Finkel, J. Duc, E. R. Fearon, C. V. Dang, G. F. Tomaselli, *J. Biol. Chem.* **268**, 5 (1993)].
28. We thank J. Griner, B. Choi, and M. Seddon for technical support; R. Guzman for the balloon-injured rat carotid tissue; W. John Martin for the CMV-positive and CMV-negative DNA; R. Dreyfuss for the photomicrography; A. Gown for HHF35; C. Midgley for CM-1; and A. Levine for plasmids p50-2 and p11-4.

7 December 1993; accepted 13 May 1994

Mitotic Regulation of Microtubule Cross-Linking Activity of CENP-E Kinetochore Protein

Hong Liao, Gang Li, Tim J. Yen*

CENP-E is a kinesin-like protein that is transiently bound to kinetochores during early mitosis, becomes redistributed to the spindle midzone at anaphase, and is degraded after cytokinesis. At anaphase, CENP-E may cross-link the interdigitating microtubules in the spindle midzone through a motor-like binding site at the amino terminus and a 99–amino acid carboxyl-terminal domain that bound microtubules in a distinct manner. Phosphorylation of the carboxyl terminus by the mitotic kinase maturation promoting factor (MPF) inhibited microtubule-binding activity before anaphase. Thus, MPF suppresses the microtubule cross-linking activity of CENP-E until anaphase, when its activity is lost.

Chromosome segregation is a highly complex process that relies on the interactions between microtubules of the spindle and a chromosomal domain called the kinetochore. This microtubule-kinetochore connection is essential for the alignment of chromosomes to the metaphase plate as well as for their separation toward opposite ends of a dividing cell. CENP-E is a 312-kD protein that belongs to the kinesin superfamily of microtubule-based motors (*1*). The subcellular distribution of CENP-E changes markedly during the cell cycle (*1*, *2*). CENP-E is initially detected as a diffuse cytoplasmic protein in cells that are in the late stages of the cell cycle (G_2 and prophase). It is associated with the kinetochores at prometaphase, but this interaction persists only to metaphase. At anaphase, CENP-E dissociates from the kinetochores and is redistributed to a set of fibers in the spindle midzone. CENP-E becomes concentrated into the midbody at telophase and is degraded after cytokinesis. The specific localization of CENP-E at the kinetochores and the spindle midzone suggests that it may be one of the motors underlying chromosome movement as well as spindle pole elongation during anaphase B (*3*, *4*).

The localization of CENP-E to the spindle midzone during anaphase may reflect cross-linking of the overlapping microtubules within this region because CENP-E appears to

Fox Chase Cancer Center, 7701 Burholme Avenue, Philadelphia, PA 19111, USA.

*To whom correspondence should be addressed.

have at least two biochemically distinct microtubule-binding domains (2). To directly identify the microtubule-binding domains within CENP-E, six overlapping fragments that span the entire length of the protein were expressed by in vitro translation of in vitro–synthesized RNAs (5), and the translation products were tested for microtubule binding (6) (Fig. 1A). Consistent with the similarity to motor domains of kinesins, the NH_2-terminal 540 amino acids of CENP-E quantitatively bound to microtubules in the absence of adenosine triphosphate (ATP) and were extractable by ATP but not with a nonhydrolyzable analog such as β-γ-imidoadenosine 5′-phosphate (AMP-PNP) (Fig. 1B).

Microtubule binding was not observed for the fragments that encompassed amino acids 324 to 2126. However, a second microtubule-binding domain was identified within the COOH-terminal 554 amino acids of CENP-E (CENP-$E^{COOH554}$). Further analysis revealed that although microtubule binding was specified by CENP-$E^{COOH243}$, deletion of the COOH-terminal 99 amino acids from this fragment abolished microtubule binding (Fig. 1C). Fusion of CENP-E^{COOH99} to the COOH-terminus of the phage T4 gene10 leader peptide in the expression vector pET17xb produced a hybrid protein that quantitatively bound to microtubules. The gene10 leader peptide by itself did not bind to microtubules. Deletions that removed the extreme COOH-terminal 35 and 87 amino acids from this gene10:CENP-E hybrid protein abolished microtubule binding. These results show that the COOH-terminal 99 amino acids of CENP-E are necessary and sufficient for microtubule binding.

CENP-$E^{COOH554}$ was used to characterize the microtubule-binding properties of the COOH-terminus because it was important to avoid any effects that might be contributed by the gene10 peptide. Microtubule binding by CENP-$E^{COOH554}$, unlike the motor domain of kinesins, was insensitive to ATP. This property as well as the high proline content (13%) and basic isoelectric point (pI = 9.4) of CENP-E^{COOH99} are common to microtubule-associated proteins (MAPs) and tau's (7, 8). Interactions of MAPs and tau's with microtubules are disrupted at moderate salt concentrations, but microtubule binding by CENP-$E^{COOH554}$ resisted extraction by high salt concentrations (up to of 2 M NaCl) (Fig. 2A). CENP-$E^{COOH554}$ cofractionated with tubulin through two cycles of polymerization and depolymerization (Fig. 2B). When microtubules were depolymerized, CENP-$E^{COOH554}$ was quantitatively released into the supernatant, which suggests that it does not form an insoluble aggregate when bound to microtubules. After repolymerization, CENP-$E^{COOH554}$ again bound to the microtubules in a manner that remained resistant to high salt concentrations (Fig. 2B). The resistance of the interaction between CENP-$E^{COOH554}$ and microtubules to high salt concentrations

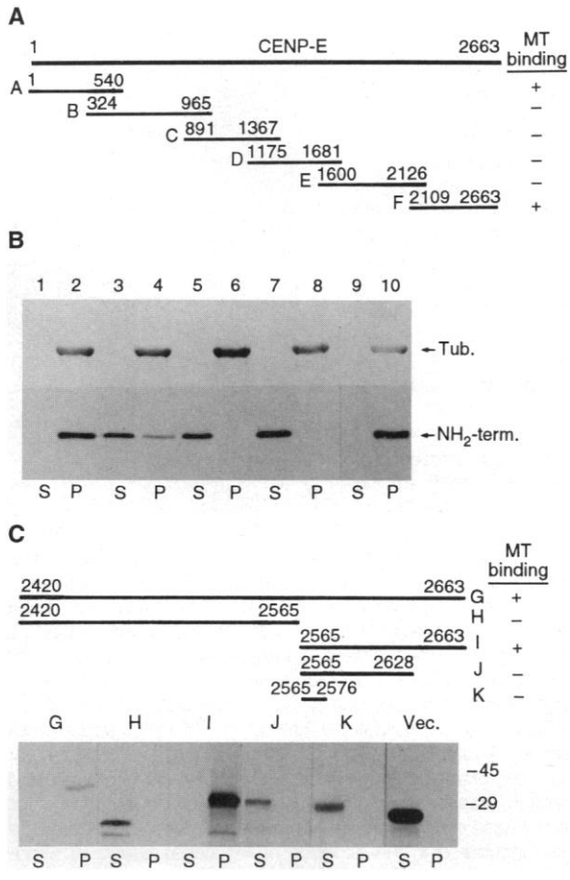

Fig. 1. Identification of two microtubule-binding domains at the NH_2- and COOH-termini of CENP-E. (**A**) Schematic representation of the fragments within CENP-E (numbers denote amino acid positions) and their in vitro microtubule-binding (MT) activity. (**B**) MT binding by the NH_2-terminal motor-like domain exhibits sensitivity to ATP. (Top) Coomassie-stained gel showing the supernatant (S) and pellet (P) fractions after MT cosedimentation experiment. Arrow points to tubulin. (Bottom) Autoradiography of the same gel showing the partitioning of the radiolabeled translation products between the S and P fractions. MT-binding reactions were done in control buffer (lanes 1 and 2), buffer with increasing concentrations of MgATP (lanes 3 and 4, 2.5 mM ATP; lanes 5 and 6, 5.0 mM ATP; lanes 7 and 8, 10 mM ATP), and 2.5 mM AMP-PNP (lanes 9 and 10). (**C**) Mapping of the COOH-terminal MT-binding domain. (Top) Schematic of the COOH-terminal fragments H to K. (Bottom) Autoradiogram showing the various in vitro translation products in the supernatant, or MT-containing pellet fractions. Fragments I, J, and K were fused to the gene10 peptide in pET17xb. Vec., the 260–amino acid gene10 translation product derived from pET17xb. Molecular size standards are indicated on the right (in kilodaltons).

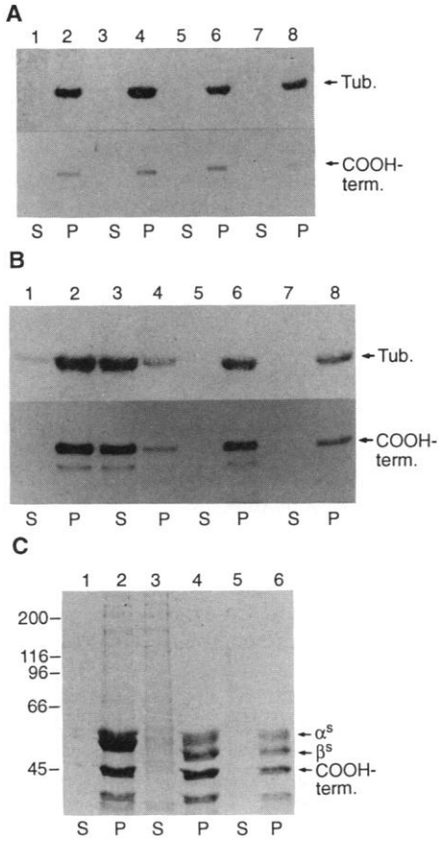

Fig. 2. Characterization of the COOH-terminal MT-binding domain of CENP-E. (**A**) MT binding by CENP-$E^{COOH554}$ resists salt extraction. No salt (lanes 1 and 2); 0.3 M NaCl (lanes 3 and 4); 1.0 M NaCl (lanes 5 and 6); and 2.0 M NaCl (lanes 7 and 8). (**B**) CENP-$E^{COOH554}$ coassembles with MT. Supernatant and pellet fractions after polymerization (lanes 1 and 2); depolymerization of the MT (lane 3 and 4); and second cycle of polymerization (lanes 5 and 6). Extraction of the twice-cycled MT with 2 M NaCl (lanes 7 and 8). The small amount of COOH-terminus in the pellet fraction (lane 4) probably reflects molecules that were bound to cold-stable microtubules. Top and bottom panels show, respectively, Coomassie staining and autoradiograms of the same gels. (**C**) Comparison of the abilities of bacterially expressed CENP-$E^{COOH368}$ and brain MAPs to bind to S-MT. Coomassie-stained gel showing supernatant (S) and pellet (P) fractions after binding CENP-$E^{COOH368}$ and MAPs to undigested MT (lanes 1 and 2) or S-MT (lanes 3 and 4). The S-MT pellet in lane 4 was extracted with 2 M NaCl and centrifuged (lanes 5 and 6). α^5 and β^5 denote subtilisin-digested tubulin subunits. Molecular size standards are indicated on the left (in kilodaltons).

is not a result of its expression in a reticulocyte translation system, because bacterially derived CENP-$E^{COOH368}$ displayed the identical properties.

To examine the COOH-terminal binding site of CENP-E along microtubules, we tested its ability to bind to subtilisin-digested microtubules (S-MT), a treatment that selectively removes the acidic COOH-terminal residues from α- and β-tubulin (*9*, *10*) and produces microtubules that can no longer bind to MAPs (*9*). We coincubated S-MT with bacterially expressed CENP-$E^{COOH368}$ and crude brain MAPs (*11*). The simultaneous inclusion of MAPs in the binding reaction provided an internal control to assess the relative amount of S-MT in our preparations. Identical results were obtained when the MAPs and CENP-$E^{COOH368}$ were incubated separately with S-MTs. Under conditions in which both MAPs and CENP-$E^{COOH368}$ were quantitatively bound to normal microtubules, only the MAPs failed to bind to S-MT (Fig. 2C). This provides functional evidence that the majority of the microtubules in these reactions were subtilisin-digested. In contrast, CENP-$E^{COOH368}$ was able to bind to S-MT in a manner that remained resistant to extraction by high concentrations of salt (Fig. 2C). Thus, the binding of CENP-$E^{COOH368}$ to a region of the microtubule lattice that is not used by conventional MAPs may contribute to differences in sensitivity to salt extraction.

The presence of microtubule-binding domains at the NH_2- and COOH-termini of CENP-E supports the ability of this protein to cross-link microtubules. In vivo, this function would be temporally regulated because the association of CENP-E with microtubules in the spindle midzone is not detected until anaphase, despite the presence of high concentrations of CENP-E prior to this time (*1*, *2*). Inspection of the CENP-E^{COOH99} microtubule-binding domain revealed consensus phosphorylation sites (SPK) (*12*) for maturation-promoting factor (MPF), a cyclin B–cdc2 kinase complex that triggers cell entry into mitosis, and that its inactivation is necessary for the transition from metaphase to anaphase. This observation was confirmed when MPF that had been purified from metaphase extracts of clam embryos (or mitotic *Xenopus* or mammalian extracts) by affinity to p13 (*13*) was able to phosphorylate CENP-$E^{COOH368}$ in vitro. Phosphorylation of this domain by MPF quantitatively inhibited its microtubule-binding activity because no detectable amounts of phosphorylated CENP-$E^{COOH368}$ were found to bind to microtubules (Fig. 3A). Inhibitory modifications of the microtubules are apparently not introduced by components from the kinase reaction, because the unphosphorylated CENP-$E^{COOH386}$ did bind to microtubules in the same reaction (Fig. 3A).

To obtain in vivo support of our in vitro findings that MPF can regulate the COOH-terminal microtubule-binding domain of CENP-E, a modified version of CENP-$E^{COOH368}$, which contained the hemagglutin (HA) epitope–tag derived from the influenza hemagglutinin protein (*14*), was expressed in HeLa cells. By labeling cells with [^{32}P]orthophosphate, we initially established that endogenous CENP-E is phosphorylated during mitosis (Fig. 3B). The transfected CENP-$E^{COOH368}$ that was extracted from M-phase cells (mitotic cells were selectively enriched by mechanical shake-off and found to be >95% at metaphase) was found to migrate more slowly than the form that was expressed in interphase cells after SDS–polyacrylamide gel electrophoresis (PAGE) (Fig. 3B). The retarded migration of the mitotic form of CENP-$E^{COOH368}$ was sensitive to phosphatase treatment, thus demonstrating that this domain of CENP-E is specifically phosphorylated during mitosis (Fig. 3B).

To verify that CENP-$E^{COOH368}$ is a substrate of MPF in vivo, we compared its two-dimensional (2D) phosphopeptide map (*15*) to one derived from the in vitro phosphory- lation. In vitro phosphorylation occurred exclusively on serine residues in three tryptic peptides (Fig. 3C). These phosphopeptides coaligned with those that were obtained from in vivo phosphorylated CENP-$E^{COOH368}$. All three phosphopeptides incorporated an equivalent amount of ^{32}P in vivo, whereas in vitro one of these peptides was preferentially labeled. The difference in labeling efficiency could result from a different conformation adopted by this domain in vivo or from the presence of associated proteins. The unique spot derived from the in vivo–labeled CENP-$E^{COOH368}$ could be due to phosphorylation by a different kinase or to a difference in the specificity of MPF.

We tested the microtubule-binding properties of the mitotic and interphase forms of the CENP-$E^{COOH368}$ by incubating lysates from transfected cells with purified microtubules (*16*). The CENP-$E^{COOH368}$ that was expressed and phosphorylated in mitotic cells failed to bind to microtubules (Fig. 3D). The ability of the interphase form of CENP-$E^{COOH368}$ to bind to microtubules was unexpected because the association of endogenous CENP-E with microtubules is not obvious during interphase. This result is probably a consequence of its expression at an inappropriate time of the cell cycle. Because most of the interphase, adherent cells expressing CENP-$E^{COOH368}$ were in the G_1 and S phases of the cell

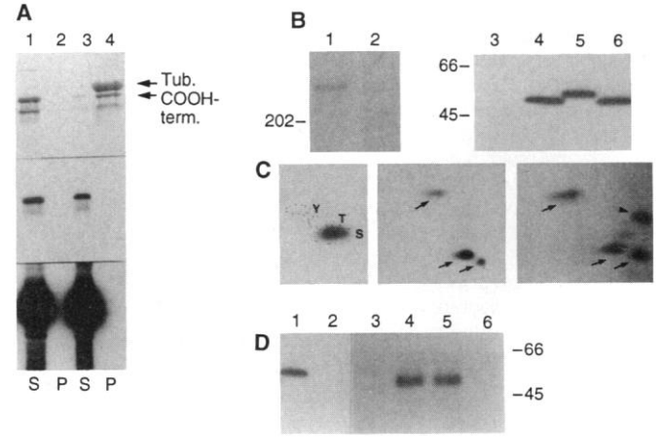

Fig. 3. Microtubule binding by CENP-$E^{COOH368}$ is inhibited by phosphorylations introduced by MPF in vitro and in vivo. (**A**) In vitro phosphorylation of CENP-$E^{COOH368}$ by MPF inhibits MT binding. Phosphorylated and unphosphorylated CENP-$E^{COOH368}$ were centrifuged in the absence (lanes 1 and 2) or presence (lanes 3 and 4) of MT. (Top) Coomassie-stained gel showing the presence of CENP-$E^{COOH368}$ in the supernatant (lane 3) and MT-containing pellet (lane 4) fractions. (Middle) Autoradiograph of the same gel. (Bottom) A one-hundred-times longer exposure of the same fractions. (**B**) CENP-E and transfected CENP-$E^{COOH368}$ are phosphorylated at mitosis. Immunoprecipitation of ^{32}P-labeled extracts from mitotic (lane 1) and interphase (lane 2) HeLa cells with antibodies to CENP-E. Detection of the HA-tagged CENP-$E^{COOH368}$ in untransfected (lane 3), transfected interphase (lane 4), transfected mitotic extracts (lane 5), and mitotic extracts after phosphatase treatment (lane 6). Molecular size standards are indicated on the left of panels (in kilodaltons). (**C**) Comparison of in vitro– and in vivo–phosphorylated CENP-$E^{COOH368}$. (Left) Phosphoamino acid analysis of in vitro–phosphorylated CENP-$E^{COOH368}$ (Y, phosphotyrosine; T, phosphothreonine; S, phosphoserine). (Middle) Phosphopeptide map of in vitro–phosphorylated CENP-$E^{COOH368}$. (Right) Phosphopeptide map of transfected CENP-$E^{COOH368}$ extracted from mitotic cells. Arrows point to the three spots that coalign; arrowhead points to unique spot. (**D**) Assay for MT binding by the transfected CENP-$E^{COOH368}$ in M-phase extracts (lanes 1 and 2) and interphase extracts (lanes 3 and 4). Interphase extracts were also incubated in the absence of MT (lanes 5 and 6). Odd- and even-numbered lanes represent supernatant and MT-containing pellet fractions, respectively. Molecular size standards are indicated on the right (in kilodaltons).

cycle, the CENP-E^{COOH368} derived from these cells would not be expected to be phosphorylated by mitosis-specific kinases and can therefore bind to microtubules.

To verify that the microtubule-binding activity of CENP-E^{COOH368} was regulated during mitosis in vivo, we examined its distribution in cells that were at different stages of mitosis and compared it with that of endogenous CENP-E (*14*). In metaphase cells, endogenous CENP-E was localized to the kinetochores of chromosomes, whereas CENP-E^{COOH368} was diffusely distributed throughout cells and did not associate with microtubules (Fig. 4, B and D). In contrast, when the CENP-E^{COOH368} was expressed at detectable levels in anaphase cells, it was prominently distributed along the microtubules in the spindle of anaphase cells (Fig. 4H). These findings confirm our model that the microtubule-binding activity of CENP-E^{COOH} is regulated during mitosis. The apparent preferential localization of the CENP-E^{COOH368} to the spindle is probably caused by the high density of microtubules in this region. It is unlikely that the CENP-E^{COOH368} displays any selectivity for any particular subset of microtubules. The distribution of CENP-E^{COOH368} along the microtubules in anaphase cells was not uniform because it is noticeably absent near the center of the spindle. Because endogenous CENP-E normally occupies this narrow zone (Fig. 4F), its presence may have interfered with the ability of the transfected CENP-E^{COOH368} to bind to this region.

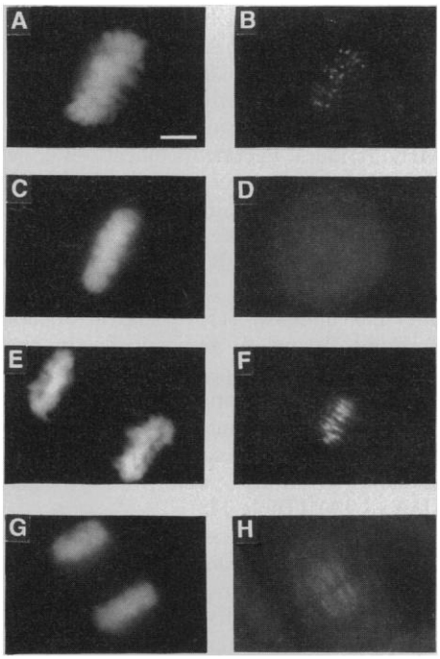

Fig. 4. Immunofluorescence detection of transfected CENP-E^{COOH368} (**D** and **H**) or endogenous CENP-E (**B** and **F**) in metaphase (B and D) and anaphase (F and H) HeLa cells. Chromosomes (**A, C, E,** and **G**) were visualized after staining with 4′,6′-diamidino-2-phenylindole (DAPI). Bar, 10 μm.

In conclusion, the identification of two biochemically distinct microtubule-binding domains at the NH_2- and COOH-termini of CENP-E support its role as a microtubule cross-linker. Microtubule cross-linking function is suppressed before anaphase by mitotic kinases such as MPF, which phosphorylates and inhibits the microtubule-binding activity of the COOH-terminus. The loss of MPF activity at the onset of anaphase (*17*) would lead to the dephosphorylation and activation of the COOH-terminal microtubule-binding domain in CENP-E. The localization of endogenous CENP-E to just a narrow strip across the spindle equator may be related to its association with kinetochores. At metaphase, alignment of the chromosomes would bring the kinetochore-associated CENP-E to a position that is equidistant between the two poles. After dissociating from the kinetochore at anaphase, CENP-E would encounter the overlapping set of antiparallel microtubules in the spindle and cross-link them through its two microtubule-binding domains. Microtubule cross-linking by CENP-E may help stabilize the overall structure of the anaphase spindle or serve to push the overlapping microtubules past each other and elongate the spindle poles.

REFERENCES AND NOTES

1. T. J. Yen *et al.*, *EMBO J.* **10**, 1245 (1991).
2. T. J. Yen, G. Li, B. T. Schaar, I. Szilak, D. W. Cleveland, *Nature* **359**, 536 (1992).
3. K. E. Sawin and J. M. Scholey, *Trends Cell Biol.* 1, 122 (1991).
4. J. R. McIntosh and M. P. Koonce, *Science* **246**, 622 (1989).
5. Constructs expressed in in vitro transcription and translation were as follows. Fragment A was amplified from CENP-E complementary DNA (cDNA) by polymerase chain reaction (PCR) with the oligonucleotides 5′-GAATTCCATATGGCG-GAGGAAGGAGC-3′ and 5′-GGATCCTCTA-GAGCCTCAAATTC-3′ to create Nde I and Bam HI restriction sites at the 5′ and 3′ ends of the PCR product. Nde I– and Bam HI–digested PCR product was ligated to the same sites in pET3a (Novagen). cDNAs that encoded the amino acids for fragments B (324–965), C (891–1367), D (1175–1681), E (1600–2126), F (2109–2663), G (2420–2663), and H (2420–2565) were excised from CENP-E cDNA and fused in-frame with the initiation codon ATG that was created by filling in the Nco I–digested ends in the vector pT7β (*18*). DNA fragments encoding the amino acids for fragments I (2565–2663), J (2565–2628), and K (2565–2576) were fused in-frame with the gene10 peptide of pET17xb (Novagen) by cloning into the Hind III site that had been treated with mung bean nuclease. The junctions of all these constructs were verified by DNA sequencing. Plasmids were linearized by cutting at a Bam HI site that was downstream of the 3′ end of the inserts and then transcribed with T7 RNA polymerase (Stratagene). Capped RNAs were then translated in rabbit reticulocyte lysate (Promega) in the presence of [^{35}S]methionine (Amersham).
6. J. T. Yang, R. A. Laymon, L. S. B. Goldstein, *Cell* **56**, 879 (1989). In vitro MT cosedimentation assay was done essentially as described. Purified tubulin was polymerized in the presence of taxol, sedimented by centrifugation at 30,000*g*, and resuspended in TMG buffer [40 mM tris-HCl (pH 7.2), 2 mM $MgCl_2$, 4 mM EGTA, 4 mM dithiothreitol (DTT), and 4 mM guanosine triphosphate]. In vitro translation products were clarified by centrifugation at 50,000*g* before incubation with MT. After the binding reaction was centrifuged at 40,000*g*, supernatant and pellet were fractionated by SDS-PAGE, stained to visualize tubulin, and then exposed to x-ray film.
7. S. A. Lewis, D. Wang, N. J. Cowan, *Science* **242**, 936 (1988).
8. G. Lee, R. L. Neve, K. S. Kosik, *Neuron* **2**, 1615 (1989).
9. L. Serrano, J. Avila, R. B. Macioni, *Biochemistry* **23**, 4675 (1984). Subtilisin digestion of microtubules was done essentially as described. The increased electrophoretic mobility of β^s tubulin has been shown to be caused by the loss of its COOH-terminal residues (*10*). Because the subtilisin-treated α-tubulin did not exhibit a substantial change in its migration in SDS-PAGE, we used two α-tubulin–specific monoclonal antibodies that recognized epitopes located either proximal to the COOH-terminus (DM1A) or at the extreme COOH-terminus (YL1/2) to determine the extent of digestion (*10*). Immunoblotting with these monoclonal antibodies revealed that limited subtilisin digestion removed only the extreme COOH-terminal residues of α-tubulin.
10. B. M. Paschal, R. A. Obar, R. B. Vallee, *Nature* **342**, 569 (1989).
11. Expression and purification of CENP-E^{COOH368} in *Escherichia coli*. A 1.3-kb Dra I cDNA fragment that encodes the COOH-terminal 368 amino acids of CENP-E was cloned into pGEX-2T (Pharmacia) at the Nco I site that had been filled in. The resultant plasmid, pGEXDraB, was transformed into BL21 host cells, and protein expression was induced with 50 μM isopropyl-β-D-thiogalactopyranoside (IPTG) for 4 hours at room temperature. Cells were resuspended in 1/10th volume of phosphate-buffered saline (PBS), incubated with lysozyme (0.1 mg/ml) for 30 min on ice, and sonicated. After centrifugation at 25,000*g* for 20 min, the supernatant was passed through a glutathione-Sepharose column (Sigma). The protein was digested with thrombin (Boehringer), and the COOH-terminus of CENP-E was eluted from the column, desalted, and concentrated in a microconcentrator (Amicon). Portions were stored at −80°C.
12. E. A. Nigg, *Trends Cell Biol.* **3**, 296 (1993).
13. A. Hershko *et al.*, *J. Biol. Chem.* **266**, 16376 (1991). p13-coupled beads were used to affinity purify MPF from fertilized surf clam *Spisula solidissima* embryo extracts that were synchronized at metaphase. Bacterially expressed CENP-E^{COOH368} (2 μg) was incubated in kinase buffer [30 mM β-glycerophosphate, 7.5 mM *p*-nitrophenyl phosphate, 12.5 mM MOPS (pH 7.2), 2.5 mM EGTA, 7.5 mM $MgCl_2$, 0.05 mM sodium vanadate, 2.5 mM DTT, 5 μM ATP and 200 μCi of [γ-^{32}P]ATP (7000 Ci/mM; ICN)] containing MPF bound to p13 beads. The reaction was incubated at 16°C for 30 min and was stopped by addition of unlabeled ATP (final concentrations, 1 mM). The reaction was centrifuged in a microconcentrator to remove unincorporated label and to concentrate the labeled protein.
14. A 1.3-kb Dra I cDNA fragment that encodes the COOH-terminal 368 amino acids of CENP-E was inserted downstream of the HA epitope–tag in the expression vector pSV2 (*19*). HeLa cells were transiently transfected by calcium phosphate precipitation (*20*). Twenty-four hours after transfection, mitotic cells were separated from interphase cells by mechanical shake-off. For in vivo labeling,

transfected cells were labeled with [^{32}P]orthophosphate (1 mCi/ml; ICN) in phosphate-free media for 3 to 4 hours before shake-off. Cells were lysed with RIPA buffer [150 mM NaCl, 50 mM tris-HCl (pH 7.5), 0.5% deoxycholate, 1.0% NP-40, 0.1% SDS, 1 mM phenylmethylsulphonyl fluoride, leupeptin, aproptinin, and pepstatin (each 1 μg/ml), and phosphatase inhibitors] and clarified by centrifugation at 15,000*g* for 10 min at 4°C. mAb 12CA5 to HA (Babco) was added to the supernatant (1:500) and incubated for 2 hours at 4°C. Antibody to mouse immunoglobulin G (IgG) coupled to agarose (Sigma) was then added to precipitate the immune complex. After the pellet had been washed, samples were boiled in SDS–sample buffer, separated by SDS-PAGE, transferred to Immobilon-P (Millipore), and probed with a rabbit polyclonal antibody (1:500 dilution) to CENP-E^{COOH368}. Bound primary antibodies were detected with ^{125}I-labeled protein A (ICN). For phosphatase treatment, precipitated beads were washed twice with RIPA and twice with alkaline phosphatase buffer and incubated with 50 U of calf intestinal phosphatase (Gibco) at 37°C for 30 min. For immunofluorescence staining, transfected cells grown on glass cover slips were fixed directly in −20°C methanol, rehydrated in PBS containing 0.1% bovine serum albumin, and incubated with either monoclonal antibody 12CA5 or antibody to CENP-E (pAb1) (*2*) followed by fluoroscein isothiocyanate–conjugated antibody to mouse or rabbit IgG (Gibco). Staining was visualized with a 100X PlanNeofluor objective using a Zeiss Axiophot microscope.

15. Phosphoamino acid analysis was done by hydrolyzing gel-purified ^{32}P-labeled protein in 6 N HCl at 110°C and separating the hydrolysate in the presence of unlabeled phosphoamino acid standards by 2D thin-layer chromatography. After electrophoresis at pH 3.5, ascending chromatography in 62.5% (v/v) isobutyric acid was used to separate the phosphoamino acids. Standards were visualized by spraying the plates with ninhydrin and then exposing the plate to film. Phosphopeptide maps were generated by digestion of ^{32}P-labeled protein with 20 μg of trypsin in 50 mM ammonium bicarbonate (pH 8.05) at 37°C overnight. Separation was carried out by electrophoresis (at pH 3.5) at 1 kV for 1.5 hours. Ascending chromatography was carried out in solvent consisting of acetic acid, pyridine, butanol, and water (1:4.9:3.2:4). Labeled peptides were detected by autoradiography and quantitated with a Fujix Bio-Imaging Analyzer (Fuji Photo).
16. MT-binding assays were done by addition of 20 μg of purified tubulin and 20 μM taxol (final concentration) to S100 extracts prepared by hypotonic lysis [10 mM tris-HCl (pH 7.0), 2 mM $MgCl_2$, and 10 mM NaCl, including protease inhibitors] of transfected cells. After incubation at 37°C for 30 min, the reaction was centrifuged and the supernatant and pellet fractions were examined for the presence of the HA-tagged CENP-E^{COOH368} by immunoprecipitation and immunoblotting as described above.
17. J. Pines and T. Hunter, *Nature* **346**, 760 (1990).
18. A. R. Krainer, T. Maniatis, B. Ruskin, M. R. Green, *Cell* **36**, 993 (1984).
19. R. C. Mulligan and P. Berg, *Proc. Natl. Acad. Sci. U.S.A.* **78**, 2072 (1981).
20. C. Chen and H. Okayama, *Mol. Cell. Biol.* **7**, 2745 (1987).
21. We are indebted to L. Cohen and J. Hittle for providing clam extracts and for advice on kinase reactions. We also thank D. Murphy and E. Holzbaur for advice on purification of brain tubulin, L. Cassemiris for providing tubulin monoclonal antibodies and for advice on making subtilisin microtubules, and B. T. Schaar for helpful discussions and suggestions. T.J.Y. is a Lucille P. Markey Scholar. Supported in part by NIH grant GM-44762-02, USPHS core grant CA-06927, the Lucille P. Markey Charitable Trust, the American Cancer Society CB-1, and an appropriation from the Commonwealth of Pennsylvania.

27 January 1994; accepted 19 May 1994

Importance of Peptide Amino and Carboxyl Termini to the Stability of MHC Class I Molecules

Marlène Bouvier and Don C. Wiley*

An influenza virus matrix peptide in which either the charged amino or carboxyl terminus was substituted by methyl groups promoted folding of the class I human histocompatibility antigen (HLA-A2). A peptide modified at both termini did not promote stable folding. The thermal stability of HLA-A2 complexed with peptides that did not have either terminus was ~22°C lower than that of the control peptide, whereas matrix peptide in which both anchor positions were substituted by alanines had its stability decreased by only 5.5°C. Thus, the conserved major histocompatibility complex class I residues at both ends of the peptide binding site form energetically important sites for binding the termini of short peptides.

The three-dimensional structure determination of the human major histocompatibility complex (MHC) class I molecule HLA-A2 shows that both ends of the peptide binding site are composed of polar residues conserved among all human and murine class I sequences (*1–3*). The conserved MHC residues form hydrogen bonds with polar main chain atoms of the peptide NH_2- and COOH-termini (Fig. 1) (*2, 3*). These hydrogen bonds were revealed in x-ray structures of class I molecules complexed with single viral peptide 8-mers (*4, 5*), 9-mers (*5–8*), and 10-mers (*6*) and with a mixture of endogenous peptides of various lengths (*9*).

The network of hydrogen bonds between conserved MHC class I residues and peptide NH_2- and COOH-termini appears to provide a peptide sequence–independent mode of binding for short peptides (*8, 10*). Interactions between polymorphic MHC residues in pockets along the binding site and a few peptide anchor residues provide a peptide sequence–dependent mode of binding (*3–9, 11, 12*). The two or three peptide anchor residues define class I allele–specific sequence motifs (*13–16*). Estimates of binding energies contributed by peptide sequence–specific interactions have been made for several alleles by structural comparisons of three allele-specific pockets (*12*) and by residue substitutions at anchor and non-anchor positions (*13, 14, 17*). However, similar estimates that compare the relative energetic contributions of the peptide termini and of the side chains at anchor positions have not been made. Here, we assess the importance of the NH_2- and COOH-termini of an influenza virus matrix peptide by substituting the charged groups by CH_3 groups and compare the effect of these modifications on the thermal stability of HLA-A2 complexes with those of substituting anchor positions 2 and 9 by alanines.

Because a substitution in the influenza virus matrix peptide (WT), GILGFVFTL (*18–20*), of Leu by Ala at position 9 (L9A) was found to have a negligible effect on the thermal stability of the complex (Table 1), the desired modifications at the peptide NH_2- and COOH-termini were made to L9A, rather than to WT peptide, for synthetic reasons (*21*). At the NH_2-terminus of L9A, the NH_2 group of Gly (Fig. 1, large blue atom) was substituted by a CH_3 group, G1-Ndel (Table 1), which was predicted to eliminate two hydrogen bonds (Fig. 1) to the conserved MHC residues Tyr^7 and Tyr^{171}. At the COOH-terminus of L9A, the COOH group of Ala (Fig. 1, large red atoms) was substituted by a CH_3 group, A9-Cdel (Table 1), which was expected to eliminate four hydrogen bonds (Fig. 1) to MHC residues. Peptide modifications done at either terminus retained the hydrogen and methyl side chains of Gly and Ala, respectively (Table 1). Peptide G1-Ndel+A9-Cdel combined both terminal modifications (Table 1). The optimal residues Leu and Val (*15*), found at anchor positions 2 and 9, respectively, in the HLA-A2–restricted peptides, were substituted in the WT peptide individually (I2L and L9V) and in combination (I2L+L9V) (Table 1). Alanine substitutions at both anchor positions were also made (I2A+L9A) (Table 1).

HLA-A2 complexes were reconstituted from human heavy chain and β_2-microglobulin (β_2M) expressed in *Escherichia coli* in the presence of excess peptide and purified by gel filtration chromatography (Fig. 2A) (*22*). Peptides modified at either terminus (G1-Ndel and A9-Cdel) promoted folding of HLA-A2, but a peptide modified at both termini (G1-Ndel+A9-Cdel) did not promote stable folding and was indistinguishable from the no-peptide control (Fig. 2A). A peptide having both anchor positions substi-

M. Bouvier, Department of Biochemistry and Molecular Biology, Harvard University, Cambridge, MA 02138, USA.
D. C. Wiley, Department of Biochemistry and Molecular Biology, Harvard University, and Howard Hughes Medical Institute, 7 Divinity Avenue, Cambridge, MA 02138, USA.

*To whom correspondence should be addressed.